Design Equations for BLDC Permanent Magnet Generators

Albert Hartman and Wendy Lorimer, Performance Magnetics

***Abstract*— Brushless DC machines utilizing high energy neodymium magnets are commonly used as generators to produce electricity and provide braking torques to a shaft. In this paper, we develop a set of design equations for three-phase generators with diode rectification. We define figures of merit beyond the traditional motor constant, K_m, to be used in conjunction with a FEA magnetic field solution for optimizing generator dimensions.**

I. Introduction

Brushless DC permanent magnet generators are popular for generating electricity in energy-harvesting applications. Generators utilizing high-energy rare-earth magnets can be very compact and produce useful levels of power from input sources that naturally operate at relatively low speeds. These generators can be optimized using FEA techniques, provided appropriate figure(s) of merit and performance metrics are utilized as design objectives and constraints.

A BLDC generator for energy-harvesting was designed to produce 50-200 watts at shaft speeds of 500-1300 rpm. FEA techniques were used to optimize the dimensions with a target motor constant K_m selected according to (1). Equation (1) represents generator output when speeds are low enough so that inductance can be ignored.

$$P_{load} = \omega_m^2 K_m^2 \cdot \eta(1-\eta) = \left(\frac{2}{p}\omega_e\right)^2 K_m^2 \cdot \eta(1-\eta) \qquad (1)$$

$$\text{where:} \quad \eta = \frac{R_{load}}{R_{coil} + R_{load}}$$

The machine was fabricated and performance testing was undertaken. Static torque constant and coil resistance measurements were consistent with FEA-computed values. Table I summarizes simulation and measured design parameters. At the target design speed, however, generator output power fell short of expectations predicted by (1). When driving loads were applied to characterize generator torque and current vs. speed, another departure from expected behavior was observed.

At fixed load, higher applied torques caused operating speed to increase, while output power and current increased and eventually plateaued. Beyond a critical applied torque, however, all apparent generator braking resistance suddenly disappeared and uncontrolled runaway shaft speed occurred.

The analysis in this paper describes the observed behavior. We begin with a simple single-phase circuit model (section A), extend to 3-phases with rectification (section B), and finally develop a set of design equations (section C). We conclude with recommended figures of merit for FEA-based generator optimization (section D).

TABLE I - Generator parameters

	Simulation	Measurement
Parameter	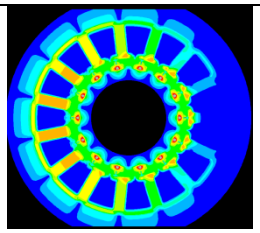	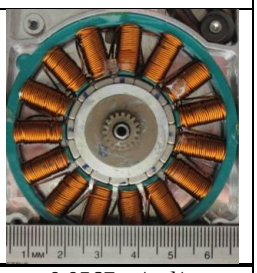
ke (phase)	0.0489 v/rad/s	0.0567 v/rad/s
resistance (phase)	0.272 ohm	0.3 ohm
inductance (phase)	0.46 mH	0.555 mH
K_M	0.115	0.127
# poles	16	

II. Analysis of BLDC Generators

Brushless DC generators are commonly characterized by their back emf constant, k_e (2) and winding resistance, R_{coil}. These parameters determine the motor constant, K_m, an established winding-independent figure of merit (3).

$$V = k_e \omega_m = k_e \frac{2}{p} \omega_e \tag{2}$$

$$K_m = {k_e}/{\sqrt{R_{coil}}} \tag{3}$$

Modeling a generator by these parameters alone is insufficient to explain the observed torque behavior. The coil inductance L_{coil} must be considered.

A. Single-Phase Generator Analysis

Table II summarizes the nomenclature used in section A. A single-phase generator can be modeled by the circuit shown in Fig. 1. Equation (4) describes the circuit behavior.

TABLE II – Nomenclature for Section A

symbol	quantity	units
k_e	back emf constant	v/rad/s
K_m	motor constant	Nm/watt$^{1/2}$
ω_m	mechanical speed	rad/s
ω_e	electrical speed	rad/s
R	resistance	ohm
L	inductance	henry
p	# poles	
I	current	amp
P	power	watts
T	torque	Nm
η	efficiency	

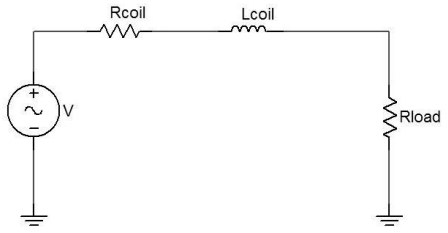

Fig. 1. Circuit representation of a single-phase generator.

$$V(t) = k_e \omega_m \sin(\omega_e t) = k_e \frac{2}{p} \omega_e \sin(\omega_e t) = IR + L\frac{dI}{dt} \tag{4}$$

$$\text{where:} \quad R = R_{coil} + R_{load}$$

Solutions for instantaneous current, torque, and output power are given by (5), (6) and (7), respectively. Time waveforms are shown in Fig. 2.

$$I(t) = \frac{2k_e\omega_e(R\sin(\omega_e t) - L\omega_e \cos(\omega_e t))}{p(R^2 + (\omega_e L)^2)} \tag{5}$$

$$T(t) = \frac{2k_e^2\omega_e \sin(\omega_e t)(R\sin(\omega_e t) - L\omega_e \cos(\omega_e t))}{p(R^2 + (\omega_e L)^2)} \tag{6}$$

$$P_{load}(t) = \frac{4{k_e}^2{\omega_e}^2 R_{load}}{p^2(R^2 + (\omega_e L)^2)^2} \cdot (R\sin(\omega_e t) - L\omega_e \cos(\omega_e t))^2 \tag{7}$$

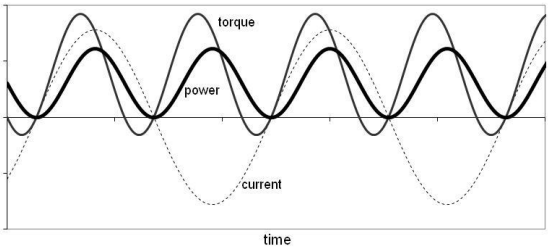

Fig. 2. Single-phase generator current, torque and power waveforms

Averaging the torque and output power over the full cycle results in (8) and (9).

$$\bar{T} = \frac{\omega_e}{2\pi}\int_0^{\frac{2\pi}{\omega_e}} T(t)dt = \frac{{k_e}^2\omega_e R}{p(R^2 + (\omega_e L)^2)} \tag{8}$$

$$\bar{P}_{load} = \frac{\omega_e}{2\pi}\int_0^{\frac{2\pi}{\omega_e}} P(t)dt = \frac{2{k_e}^2{\omega_e}^2 R_{load}}{p^2(R^2 + (\omega_e L)^2)} \tag{9}$$

With increasing speed, the magnitudes of the current and power waveforms increase and approach an upper limit. Torque, however, increases to a maximum, then begins to fall. The maximum torque occurs at a critical speed (10). The magnitude of the current and average output power at critical speed are given by (11) and (12). Power at critical speed is exactly half its high-speed limiting value; current is $1/\sqrt{2}$ times its high-speed limit.

$$\bar{T}^* = \frac{k_e^2}{2pL}$$
$$at\ {\omega_e}^* = \frac{R}{L};\ {\omega_m}^* = \frac{2R}{pL} \tag{10}$$

$$|I(\omega_e^*)| = \frac{\sqrt{2}k_e}{pL} \tag{11}$$

$$\bar{P}_{load}(\omega_e^*) = \frac{k_e^2 R_{load}}{p^2 L^2} \tag{12}$$

For a particular generator, the maximum torque is independent of both winding and load resistances. Fig. 3 shows torque versus speed behavior for various load resistances. All curves have the same maximum value. Altering the load resistance only changes the speed at which

peak torque occurs. Application of torques above the limit will cause uncontrolled acceleration.

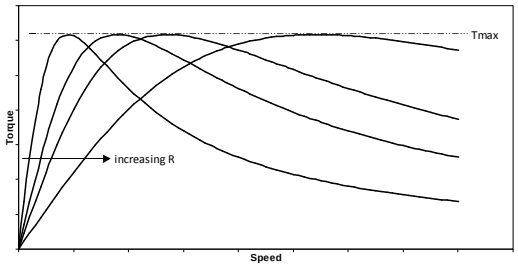

Fig 3. Effect on Braking Torque vs. Speed as resistance is changed

Recognizing that inductance plays a critical role in generator performance, we propose a supplementary figure of merit K_L as defined by (13). Like its counterpart K_m, K_L is winding-independent. For a fixed coil volume, R_{coil} and L_{coil} are both proportional to number of turns squared, while back emf constant k_e is proportional to number of turns. Consequently, not only is the maximum torque T^* independent of load resistance, it is also independent of the number of turns.

$$K_L = {k_e}\Big/{\sqrt{L_{coil}}} \tag{13}$$

Winding-independent generator metrics K_m and K_L provide useful guidance when sizing a generator for a particular application. Equation (1) predicts power output at low speed, i.e., $L\omega_e \to 0$. Equation (14) gives the maximum controllable torque the generator can sustain.

$$\bar{T}^* = \frac{K_L^2}{2p} \tag{14}$$

Returning to Fig. 2, we observe current, power, and torque waveforms are sinusoidal, characterized by a magnitude, frequency, phase, and dc-offset. Thus, we rewrite (5)-(7), as (15)-(17). Power (17) is a double frequency waveform with minimum value equal to zero. Torque is also a double frequency waveform, but has a dc offset and phase shift relative to the current waveform.

$$I(t) = \frac{2k_e\omega_e}{p\sqrt{R^2+(\omega_e L)^2}} \cdot \sin(\omega_e t - \alpha) \qquad where\ \alpha = tan^{-1}\left(\frac{\omega_e L}{R}\right) \tag{15}$$

$$T(t) = \frac{Rk_e^2\omega_e}{p(R^2+(\omega_e L)^2)} - \frac{k_e^2\omega_e}{p\sqrt{R^2+(\omega_e L)^2}}\sin(2\omega_e t+\alpha) = \frac{k_e^2\omega_e}{p\sqrt{R^2+(\omega_e L)^2}}\big(cos(\alpha) - sin(2\omega_e t+\alpha)\big) \tag{16}$$

$$P_{load}(t) = \frac{2{k_e}^2{\omega_e}^2 R_{load}}{p^2(R^2+(\omega_e L)^2)} \cdot \big(1-\cos\big(2(\omega_e t-\alpha)\big)\big) \tag{17}$$

Next, we compare uni-phase results to those of a 3-phase diode-rectified circuit.

B. Three-Phase Generator and Equivalent Uni-Phase Circuit

A common energy harvesting system utilizes a 3-phase generator and 6-diode rectifier like circuit A shown in Fig. 4.

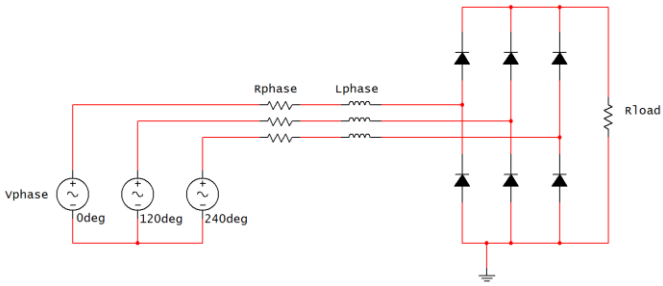

Fig. 4. Circuit A : 3-phase generator with diode rectifier

Circuit A was simulated in SPICE using parameters for the generator in Table I. SPICE simulations with ideal diodes reveal that a rectified generator is a three-phases-on device. For typical values of R, L, and V, phase currents are nearly sinusoidal, and a single phase current matches the rectified load current over a 60 degree span centered at the peak. Fig.5 shows phase current and load current in circuit A for typical generator parameters.

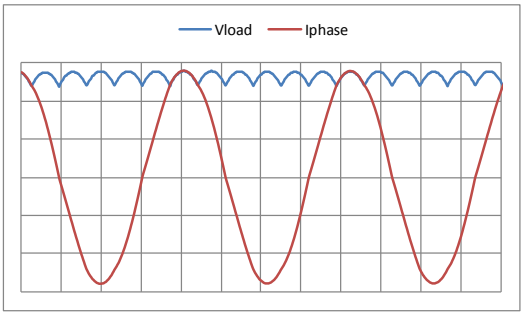

Fig. 5. Typical phase and load currents in Circuit A – all 3 phases are active throughout the cycle

We conclude the effect of diode switching is to rearrange the phases connected across the load resistor every 60 electrical degrees. Within a 60° span the circuit topology is unchanged, and can be represented by circuit B shown in Fig. 6.

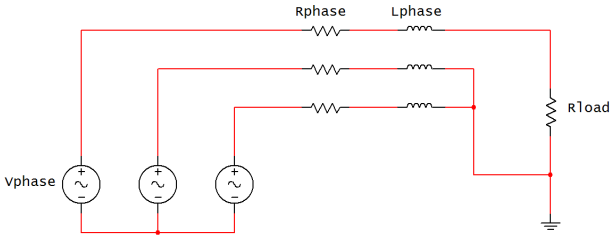

Fig. 6. Circuit B : 3-phase generator without diodes

Current in the upper phase of circuit B closely matches the phase current for the diode-rectified circuit A. The agreement

is within 0.5% for typical generator values. Currents in the other two phases of circuit B (those connected in parallel to the load resistor) are different in magnitude from each other and not in phase.

The analytical solution for current through the load resistor of circuit B is sinusoidal of magnitude given by (18).

$$|I_{load}| = \frac{3V_{phase}}{\sqrt{\left(3R_{phase} + 2R_{load}\right)^2 + \left(3L_{phase}\omega_e\right)^2}} \tag{18}$$

This solution suggests the construction of equivalent circuit C shown in Fig. 7. Circuits B and C produce identical load current.

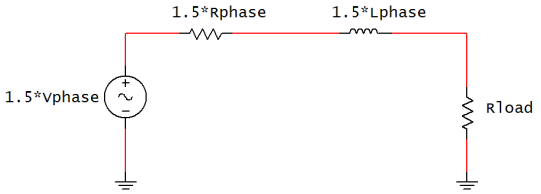

Fig 7. Circuit C : equivalent uni-phase model to circuit B (same I_{load})

Provided phase current waveforms remain sinusoidal, the current flowing in equivalent circuit C provides a good approximation to phase current in a 3-phase diode-rectified generator (Fig. 8). The other two phase currents are identical, just shifted 120 degrees.

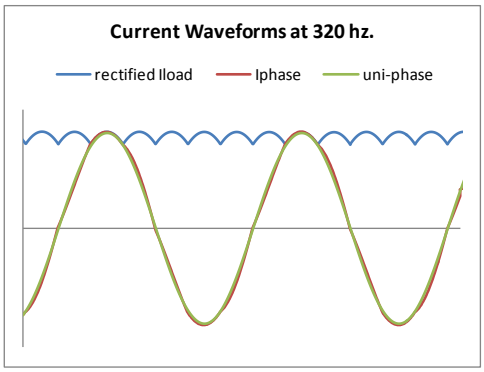

Fig. 8. Uni-phase equivalent (circuit C) compared to SPICE rectified circuit A at high ωL (sinusoidal phase current)

At low inductance or low speed (ω_eL small), rectified phase currents in circuit A at not sinusoidal (Fig. 9). Under these conditions, we would not necessarily expect circuits A, B, and C to produce similar load current. However, SPICE results show that they are close enough to accept results of circuit C integrated over 60 deg to be a reasonable approximation to 3-phase diode-rectified circuit A.

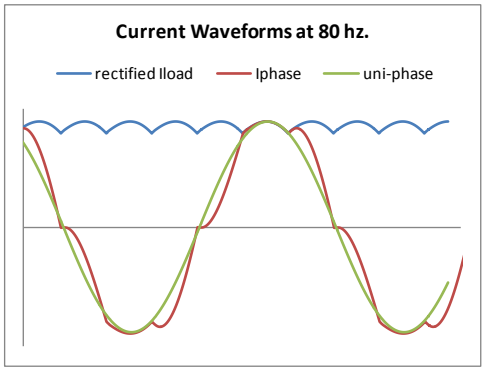

Fig. 9. Uni-phase compared to SPICE rectified circuit at low ωL (non-sinusoidal phase current)

C. *Three-Phase Rectified Generator Design Equations*

Using equivalent circuit C to approximate phase currents in a rectified generator, we develop a set of generator design equations. The equations use per-phase generator parameters as defined in Table III.

TABLE III – NOMENCLATURE FOR SECTION C

symbol	quantity	units
k_e	phase back emf per mechanical speed (ct-L)	v/rad/s
ω_m	mechanical speed	rad/s
ω_e	electrical speed	rad/s
R_{ph}	phase resistance (ct-L)	ohm
L_{ph}	phase inductance (ct-L)	henry
p	# poles	

Circuit C phase current is given by (19) and average rectified load current is given by (20).

$$I_{ph}(t) = \frac{2(1.5k_e)\omega_e}{p\sqrt{\left(1.5R_{ph} + R_{load}\right)^2 + \left(1.5L_{ph}\omega_e\right)^2}} \cdot \cos(\omega_e t) \tag{19}$$

$$\begin{aligned} \bar{I}_{load} &= \frac{3\omega_e}{\pi} \int_{-\frac{\pi}{6\omega_e}}^{\frac{\pi}{6\omega_e}} I_{ph}(t)dt \\ &= \frac{9k_e\omega_e}{\pi p\sqrt{\left(1.5R_{ph} + R_{load}\right)^2 + \left(1.5L_{ph}\omega_e\right)^2}} \end{aligned} \tag{20}$$

Average power delivered to the load resistor is formed from the topmost 60° interval of the sinusoidal load current squared (21).

$$\begin{aligned} \bar{P}_{load} &= \frac{3\omega_e}{\pi} \int_{-\frac{\pi}{6\omega_e}}^{\frac{\pi}{6\omega_e}} R_{load}\left(I_{ph}(t)\right)^2 dt = \\ &= \frac{9\left(3\sqrt{3} + 2\pi\right)R_{load}k_e^2\omega_e^2}{\pi p^2\left(9\left(R_{ph}^2 + L_{ph}^2\omega_e^2\right) + 12R_{ph}R_{load} + 4R_{load}^2\right)} \end{aligned} \tag{21}$$

Maximum output power can be achieved by selecting R_{load}

according to (22).

$$R^*_{load} = \frac{3}{2}\sqrt{R^2_{ph} + L^2_{ph}\omega^2_e} \tag{22}$$

Power consumed in the phase windings is the sum of the three sinusoidal phase currents squared times the phase resistance. The result is constant in time (23).

$$\bar{P}_{ohmic} = \frac{3}{2}R_{ph}\left|I_{ph}(t)\right|^2 = \frac{54R_{ph}k^2_e\omega^2_e}{p^2\left(9\left(R^2_{ph} + L^2_{ph}\omega^2_e\right) + 12R_{ph}R_{load} + 4R^2_{load}\right)} \tag{23}$$

Average torque and generator efficiency are given by (24) and (25), respectively.

$$\bar{T}\cdot\omega_m = \bar{P}_{load} + \bar{P}_{ohmic}$$

$$\bar{T} = \frac{9k^2_e\omega_e\left(\left(3\sqrt{3}+2\pi\right)R_{load} + 6\pi R_{ph}\right)}{2\pi p\left(9\left(R^2_{ph} + L^2_{ph}\omega^2_e\right) + 12R_{ph}R_{load} + 4R^2_{load}\right)} \tag{24}$$

$$\eta = \frac{\bar{P}_{load}}{\bar{P}_{load} + \bar{P}_{ohmic}} = \frac{\left(3\sqrt{3}+2\pi\right)R_{load}}{\left(3\sqrt{3}+2\pi\right)R_{load} + 6\pi R_{ph}} \tag{25}$$

Using Table I generator parameters and a load resistance of 1 ohm, equations (20)-(24) predict current, power, and torque shown in Figs. 10, 11 and 12, respectively. Fig. 13 shows how the equations compare to SPICE over a wide speed range. The largest discrepancy is in the ohmic losses at low speed where the phase currents are not sinusoidal. Overall, the correlation is good.

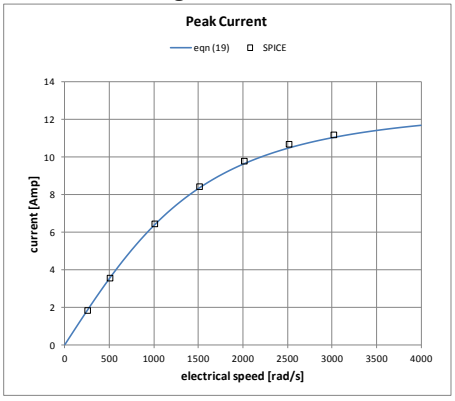

Fig 10. Load current equation (19) vs. speed compared to SPICE rectified model

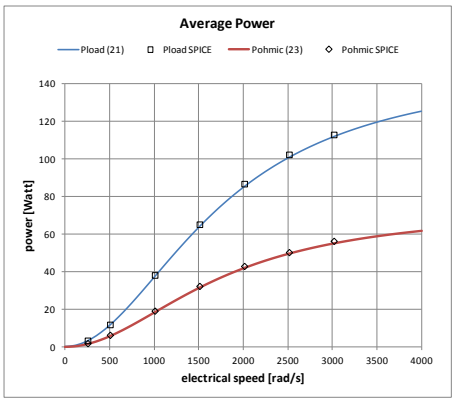

Fig 11. Average power equations (21),(23) vs. speed compared to SPICE rectified model

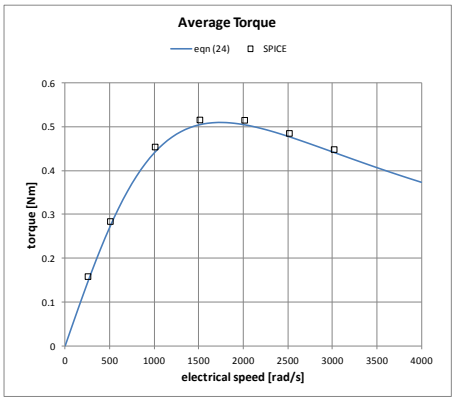

Fig 12. Average torque equation (24) vs. speed compared to SPICE rectified model

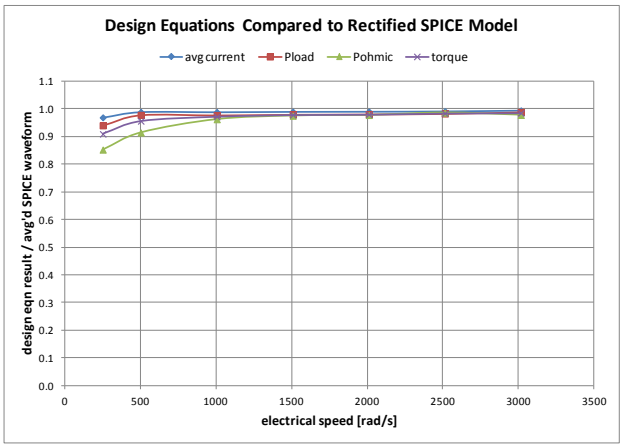

Fig 13. Design equations compared to SPICE simulation results vs. speed

Rectified current, power and torque curves are similar to the uni-phase case. Load current and power increase with speed and approach limiting values. Torque rises to a maximum at a critical speed, then declines. The value of the maximum torque is given by (26). The phase angle between back emf and phase current at ω* is 45°. Unlike the uni-phase result (10), resistance appears in the three-phase T* equation. Peak torque is actually a function of the ratio R_{load}/R_{ph}, but the dependence is weak, declining less than 9% from shorted

output to infinite load resistance (Fig. 14). If we choose $R_{load}/R_{ph} = 1/2\left(3\sqrt{3}/2\pi + 1\right) = 0.9135$, the resistance terms cancel, and we can approximate T* as (27).

$$\bar{T}^* = \frac{3k_e^2}{4\pi p L_{ph}} \frac{\left(\left(3\sqrt{3}+2\pi\right)R_{load} + 6\pi R_{ph}\right)}{2R_{load} + 3R_{ph}} \quad (26)$$

$$at\ \omega_e{}^* = \frac{2R_{load} + 3R_{ph}}{3L_{ph}}$$

$$\bar{T}^* \approx \frac{3k_e^2}{2pL_{ph}} \quad (27)$$

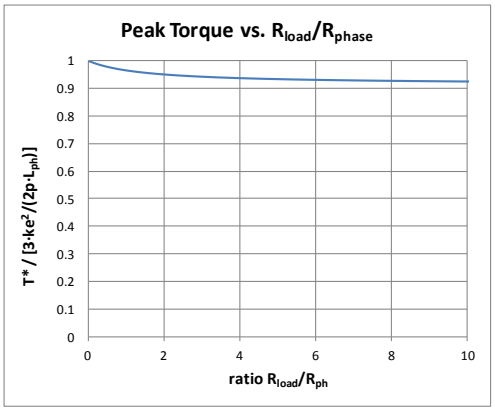

Fig 14. Weak dependence of peak torque T* on resistance ratio

Current and power at critical speed are given by (28) and (29). As in the uni-phase case, power at critical speed is exactly half its high-speed limiting value; current is $1/\sqrt{2}$ times its high-speed limit.

$$|I(\omega_e^*)| = \frac{\sqrt{2}ke}{pL_{ph}};\ \ \bar{I}(\omega_e^*) = \frac{3\sqrt{2}ke}{\pi p L_{ph}} \quad (28)$$

$$\bar{P}_{load}(\omega_e^*) = \frac{\left(3\sqrt{3}+2\pi\right)R_{load}k_e^2}{2\pi p^2 L_{ph}^2} \quad (29)$$

The transition from two-phases-on (low speed / non-sinusoidal phase current) to three-phases-on (high speed / sinusoidal phase current) is determined by the circuit L/R. If we compute the speed at which the L/R time constant (30) coincides with the rectification interval (1/6 electrical period), we get (31). This transition speed is precisely π/3 times ω*. We conclude that the critical (peak torque) speed coincides with the transition from non-sinusoidal to purely sinusoidal phase currents.

$$\tau = \frac{1.5L}{R_{load} + 1.5R_{ph}} \quad (30)$$

$$\omega = \frac{\pi\left(2R_{load} + 3R_{ph}\right)}{9L_{ph}} \quad (31)$$

D. Figure of Merit for Generator Design

In the past, we neglected inductance, and used motor constant as the sole figure of merit in generator design. Since K_m is winding-independent, it was useful in comparing machines of different types wound for different output voltages. In design, it allowed optimizing generator dimensions without pre-selecting the # turns. A typical design proceeded as follows:

- select efficiency η, spin speed ω_m, and target output power, P_{load}
- use (1) to determine the required motor constant K_m
- use ANSYS to compute K_m for different topologies and dimensions; optimize
- when optimization is complete, wind the machine to deliver power at the desired voltage

We seek a form similar to (1) that accounts for inductance and rectification. Combining (21) and (25), we can derive that form. The equation is more complicated, but it remains winding-independent, and lends itself to design procedures used in the past. Two different forms of the equation are presented.

Defining a to be the ratio of load to phase resistance (32), efficiency can be expressed as (33). Substituting (32) for Rload in (21) gives the new design equation (34). Motor constant appears, as before, but the efficiency dependence becomes a more complicated, and phase L/R ratio appears. For design, choose desired efficiency, spin speed, and target output power, then optimize according to (32) with ANSYS-calculated variables Km and Lph/Rph.

$$R_{load} = a \cdot R_{ph} \quad (32)$$

$$\eta = \frac{\left(3\sqrt{3}+2\pi\right)a}{\left(3\sqrt{3}+2\pi\right)a + 6\pi};\quad a = \frac{6\pi}{\left(3\sqrt{3}+2\pi\right)}\frac{\eta}{(1-\eta)} \quad (33)$$

$$\bar{P}_{load} = \frac{9\left(3\sqrt{3}+2\pi\right)\omega_e^2}{\pi p^2}\frac{k_e^2}{R_{ph}}\frac{a}{(3+2a)^2 + \left(3\frac{L_{ph}}{R_{ph}}\omega_e\right)^2} \quad (34)$$

Alternatively, we can express R_{load} as a function of efficiency and R_{phase} (35), eliminate R_{load}, and simplify to (36). The new parameter D appears in the denominator and is a function of both efficiency and phase L/R.

$$R_{load} = \frac{6\pi\eta R_{ph}}{\left(3\sqrt{3}+2\pi\right)(1-\eta)} \quad (35)$$

$$\bar{P}_{load} = \frac{6\left(3\sqrt{3}+2\pi\right)^2\omega_e^2}{p^2 D}\cdot\frac{k_e^2}{R_{ph}}\cdot\eta(1-\eta) \quad (36)$$

$$\mathrm{D} = \left(3\sqrt{3}+2\pi\right)^2(1-\eta)^2\left(1+\left(\frac{L_{ph}}{R_{ph}}\omega_e\right)^2\right) + 8\pi\eta(1-\eta)\left(3\sqrt{3}+2\pi\right) + 16\pi^2\eta^2$$

III. Conclusions

The behavior of three-phase brushless DC generators with diode rectification is closely modeled by the equations presented in this paper. Although the analysis relies on a simple model and assumes the generator operates as a three-phases-on device, it is accurate over a wide speed range, including low speeds, when generator phase currents are not sinusoidal.

When designing a generator, inductance must be considered because it limits output power and sets the maximum torque the machine can sustain. This is true for uni-phase as well as three-phase rectified generation.

A winding-independent metric that includes L/R as well as K_m has been derived for use in ANSYS optimization. In general, high motor constant and low inductance are desirable characteristics.

IV. Open Items and Future Work

In practice, diodes have a forward voltage drop and loads are not purely resistive, e.g., battery charging at constant voltage with ESR. Both effects could be incorporated in this model by modifying the load. Conclusions and figures of merit still apply; only the interpretation of R_{load} will to change.

Our derivation assumes flux linkages are independent of speed (no eddy currents), sinusoidal in rotation angle, and independent of current. For deep saturation and/or high load current, the latter two assumptions may not be appropriate. Under these conditions, we suggest using ANSYS to calculate phase flux linkages, $\lambda=N\phi$, as functions of position and current. Back emf, $ke(\theta,I)$, and inductance, $L(\theta,I)$, would be computed as $d\lambda/d\theta$ and as $d\lambda/dI$, respectively. A transient solution to the equivalent circuit could be obtained using MATLAB or Simulink.